ISEF 2005 - XII International Symposium on Electromagnetic Fields
in Mechatronics, Electrical and Electronic Engineering
Baiona, Spain, September 15-17, 2005

Structure-Dynamic Simulation of an Induction Machine with Eccentrically Positioned Squirrel-Cage Rotor

C. Schlensok, M. Herranz Gracia, and K. Hameyer

Institute of Electrical Machines, RWTH Aachen University
Schinkelstraße 4, D-52062 Aachen, Germany
Christoph.Schlensok@iem.rwth-aachen.de

***Abstract** – Due to the manufacturing-process tolerances of mechanical components of electrical machines the rotor can be positioned eccentrically. Either the bearings allow for displacement or the rotor itself is not con-centric with the shaft axis. In the studied case of an Induction Machine with squirrel-cage rotor (IM) an eccentrically positioned rotor results in additional net-force and vibrations. Therefore, the IM applied as power-steering drive is simulated by a structure-dynamic finite-element model to estimate the effect of eccentricity to vibration of the entire mechanical structure.*

Introduction

Many efforts have been focused on the electromagnetic behavior of eccentric induction machines with squirrel-cage rotor (for example: [1]-[3]). The unbalanced magnetic pull has been main subject to investigations regarding the behavior of torque, net-force, and surface-force density. Predictions of how the different force-excitations effect the vibration of an IM are very difficult, due to the fact that it is analytically is nearly impossible to take the geometry and the mechanical structure of the IM into account in detail. Measurements on the other hand give rather weak information of the behavior of eccentric machines, since it is difficult to control the displacement of the rotor exactly and therefore parasitic effects can hardly be detected. A slight imprecision may lead to huge errors. Therefore, the numerical simulation of the vibrations of an eccentric IM is of particular interest. It allows to consider the behavior of the IM due to eccentricity as a sole effect. Nevertheless, measurements need to be performed to verify the simulation results.

Definition of Eccentric Cases

Fig. 1 shows the three different types of eccentricity. Usually the centric case from Fig. 1(a) is subject to research. Rotor, stator, and rotational axis share the same center point. The air gap is of constant width along the circumference.

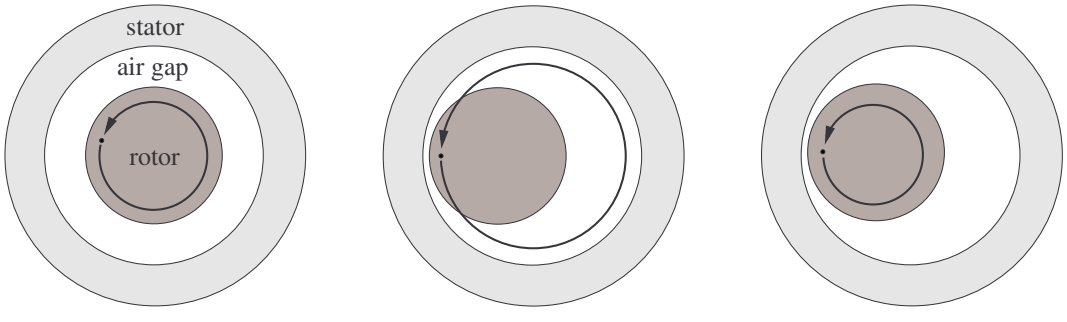

a) Centric. b) Dynamic. b) Static.

Fig. 1: Types of Eccentric Rotor Positioning.

In the case of dynamic eccentricity the rotor axis is shifted to one side (Fig. 1(b)). Therefore, the rotor whirls around the stator axis which is the rotational axis. The location of the smallest air gap revolves with rotor speed resulting in extra vibrations.
For static eccentricity the rotational axis is displaced together with the rotor axis (Fig. 1(c)). The rotor revolves in place keeping the narrowest air gap stationary.
Finally the combination of both results in a mixture of revolving and stationary part of the smallest air-gap location. Depending on the amount of each the narrowest air gap keeps more stationary (large static portion) or revolves (large dynamic portion) In this paper a 50/50 mix is studied.

Electromagnetic Simulation

For the electromagnetic simulation a transient, 2-dimensional solver with a first order time-stepping algorithm is applied. The solver is part of the open-source solver-environment *i*MOOSE [4]. The point of operation is defined with $n = 1200\ \text{min}^{-1} = 20\ \text{Hz}$ and $f_1 = 48{,}96\ \text{Hz}$. The eccentricity is set to the maximum manufacturing tolerance of $v = 0{,}1$ mm. As described in a previous paper [5] the torque of the IM is not affected significantly by eccentricity. All three models result in the same mean torque value $\overline{T} = 4.34$ Nm.
As Fig. 2 depicts, the force behavior of the three eccentric cases differ significantly. In the case of dynamic eccentricty the force points into the direction of the minimal air-gap. Therefore, it revolves with rotor speed. It has an average value of $\overline{F}_{dyn} = 170.2\ \text{N}$ pulsating due to the slotting. For the static case the force pulsates with rotor speed $f_R = 20\ \text{Hz}$ resulting in an average of $\overline{F}_{stat} = 107.4$ N. Dynamic-static eccentricity results in a mixture of the pulsating and revolving force excitation. The average is $\overline{F}_{dyn-stat} = 163.9$ N.

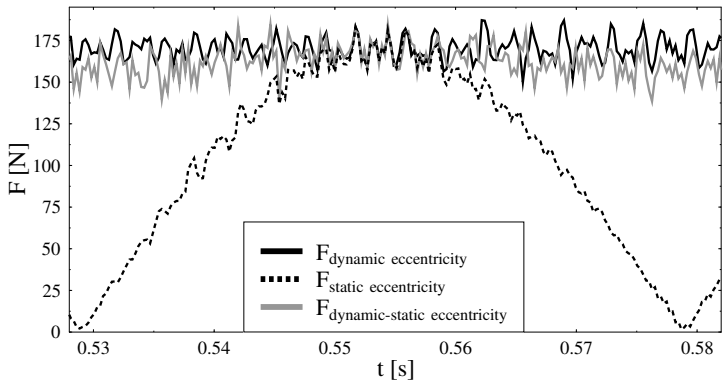

Fig. 2: Force Behavior of the Studied Eccentric Cases.

Structure-Dynamic Simulation

As input data for the structure-dynamic simulation the surface-force density acting onto the stator teeth is required. It is computed for each time step of the 2D transient electromagnetic simulation using the Maxwell-stress tensor [6]. Taking $N = 2056$ time steps into account, the surface-force density of each stator-tooth element is transformed to the frequency domain by using the Discrete Fourier Transformation (DFT) [7].
For the dynamic eccentric case (Fig. 1(a)) the spectrum of the surface-force density for a single element on the up-running edge of a stator tooth is shown in Fig. 3. The identified main orders of the air-gap field are the rotor speed $f_R = 20\ \text{Hz}$, the double stator frequency $2 \cdot f_1 = 97.92$ Hz, the first and second rotor-slot harmonic at $f_{26} = 520$ Hz and $f_{52} = 1040$ Hz with the rotor-slot number $N_R = 26$. f_{26}

and f_{52} are modulated with $2 \cdot f_1$ resulting in $f_{21} = 420$ Hz, $f_{31} = 620$ Hz, $f_{47} = 940$ Hz, and $f_{57} = 1140$ Hz. These orders and the first stator-slot harmonic at $f_{36} = 720$ Hz ($N_R = 36$) are regarded in the structure-dynamic simulation of the IM. f_R does not arise for a static eccentric rotor positioning and is reduced in the case of dynamic-static eccentricity as Fig. 4 and Fig. 5 show.

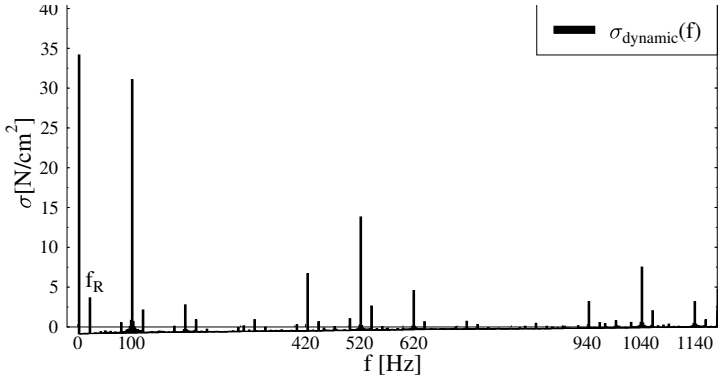

Fig. 3: Spectrum of Surface-Force Density: Dynamic Eccentricity.

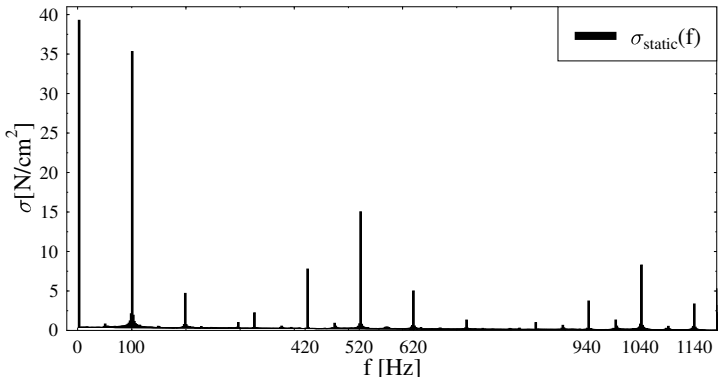

Fig. 4: Spectrum of Surface-Force Density: Static Eccentricity.

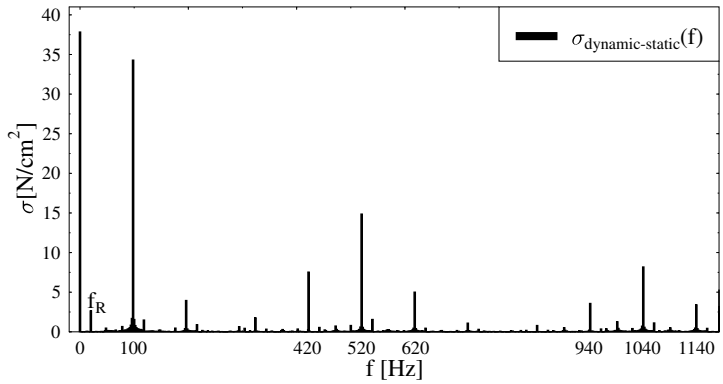

Fig. 5: Spectrum of Surface-Force Density: Dynamic-Static Eccentricity.

The surface-force density is transformed from the 2D electromagnetic model to the 3D mechanical model. The transformation algorithm produces equal total forces for each the teeth of the 2D and 3D model respectively. The discretization error is kept small by using an adequate multi-slice model for the electromagnetic 2-dimensional simulation [8].
The IM studied here is mounted on one of the two front plates. Therefore, the nodes of this face of the mechanical FE-model are fixed. Fig. 6 exemplarily shows the deformation of the stator for force

excitation at $f_R = 20$ Hz. The main mode of deformation r and its magnitude depends on the type of eccentricity. In Fig. 6(a) a significant mode of 1st order is detected for dynamic eccentricity and in the case of static eccentricity the mode is of 4th order as the cross section of the stator region depicted in Fig. 6(b) shows.

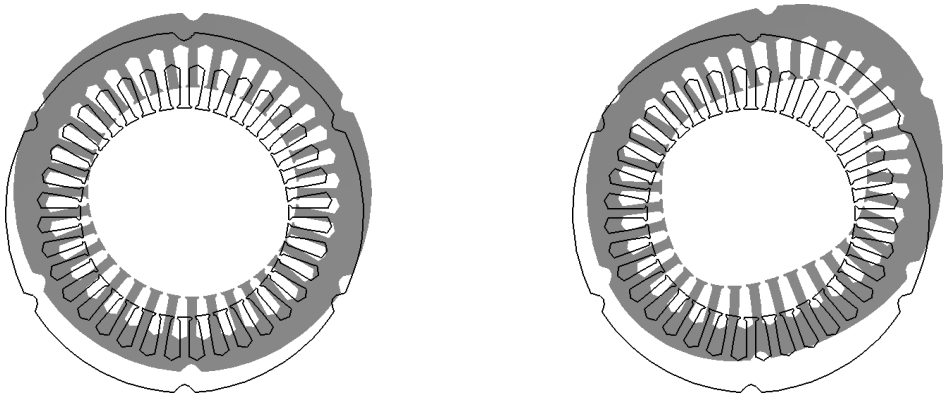

a) Dynamic Eccentricity, 20 Hz, 10.000 Times Emphasized. a) Static Eccentricity, 20 Hz, 12.000.000 Times Emphasized.

Fig. 6: Deformation Modes of the Stator for Different Types of Eccentricity at 20 Hz.

The magnitude of oscillation is very significant. As Fig. 7 shows, the magnitude of the deformation depends on the type of eccentricity. The radial component of deformation is derived from the model along a line on the circumference of the stator at $f_R = 20$ Hz. With the DFT the modes can be calculated. In the case of a significant dynamic portion of eccentricity the radial deformation is up to four dimensions higher than in the case of a centric or a static eccentric revolving rotor. In Fig. 7(a) the resulting deformation values of all four models are combined. Only those of the models with dynamic eccentric portion can be identified. They both show a strong mode of 1st order as it can be seen from Fig. 6(a) before. Fig. 7(b) shows the behavior of the deformation for the centric and static eccentric cases. The centric rotor shows a very low but dominant 4th mode. This mode can also be seen in Fig. 6(b) for static eccentricity. It is superposed by a 1st mode.

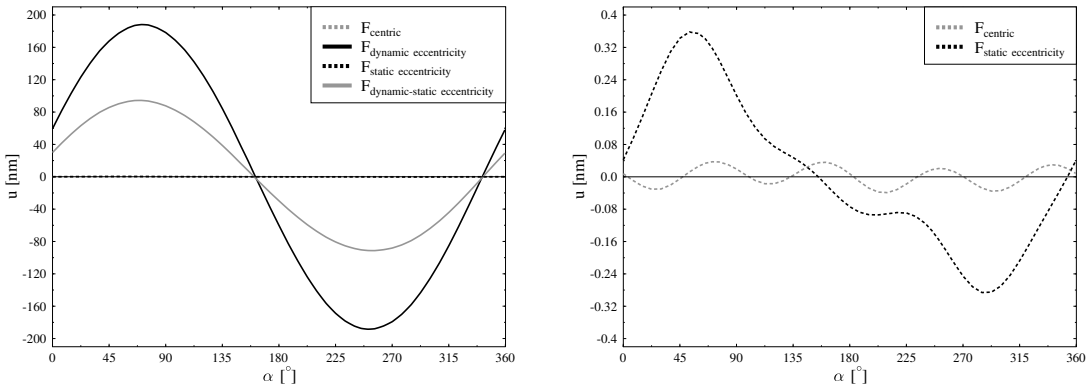

a) Deformation of All Models. b) Deformation of centric and static eccentric Model.

Fig. 7: Deformation of the Stator at 20 Hz along the Line on the Circumference.

The mode with $r = 1$ can be very harmful for the machine's mounting especially at low frequencies. This can lead to mechanical failure of the machine. Therefore, a large rate of dynamic eccentricity must be avoided.

The body sound of the IM is analyzed in the next step of the study. Therefore, the Level of the Body-Sound Index L_{BSI} is applied [8]. L_{BSI} is calculated for the housing of the IM. The structure-dynamic simulation is performed for the above mentioned, selected single frequencies. It is very time consuming to analyze the complete frequency range. The simulation of a single frequency takes approximately 3 hours. The full spectrum consists of 600 frequencies. Simulating the whole range will lead to total computational

costs of about 75 days. Therefore, measurements and analytical considerations have to be taken into account to detect the significant orders which have to be simulated.
Fig. 8 shows the level of the body-sound index for the selected frequencies for all four models. The highest levels are reached for the first stator-slot harmonic at $f_{36} = 720$ Hz although the force excitation is rather low at this frequency for all models as Fig. 3 to Fig. 5 have shown before. Here, the structure of the IM has great impact. The 36 stator teeth are easily excited to oscillate at this harmonic frequency. In any case and for any frequency eccentricity results in higher body-sound index-levels. Except for $f_R = 20$ Hz the model with exclusive static eccentric rotor produces the highest levels throughout the spectrum. On the other hand, a dynamic eccentric rotating rotor has almost no effect to the other orders regarded here.

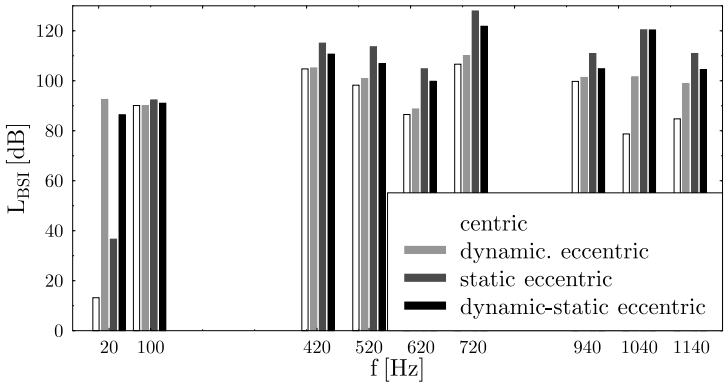

Fig. 8: Level of the Body-Sound Index for Selected Frequencies and All Models.

Taking the force excitation of the model with centric positioned rotor as reference, the difference-level of the body-sound index is calculated and analyzed. Eccentricity causes higher deformation values in any case. In the case of significant dynamic portion of eccentricity the 1st order of the rotor speed appears to be very strong (plus 70 to 80 dB). This can lead to severe mechanical damage [9]. For all the other orders regarded, the static portion of eccentricity is more critical. Raising the body-sound level up 40 dB at $f_{52} = 1040$ Hz. This frequency range is of high acoustic interest, since the human ear is very sensitive here. Therefore, static eccentricity produces extra noise which might lead to rejection of the IM during manufacturing.

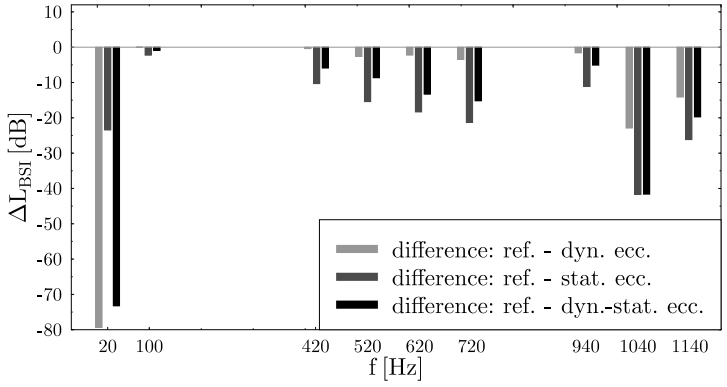

Fig. 9: Difference Level of the Body-Sound Index for Selected Frequencies and All Models.

Conclusions

For the first time the impact of different types of eccentricity to mechanical deformation of an induction machine with squirrel-cage rotor (IM) is analyzed. To do this, the Finite-Element Method (FEM) is applied. Electromagnetic, 2-dimensional models and mechanical 3-dimensional models are simulated.

The electromagnetic models take centric, dynamic and static eccentric rotor movement as well as a combination of the later two into account. The surface-force density of all four models are derived from the flux-density distribution and is analyzed in the frequency domain. As expected, a dynamic portion of eccentricity causes force excitation with the order of the rotor speed. Static eccentricity produces minor extra excitation.
The resulting frequency-dependent force excitation of the stator teeth of the IM are transformed to a structure-dynamic FE-model. This model is simulated for selected frequencies derived from measurement and analytical studies. The resulting deformation of the entire machine structure is analyzed. In the case of $f_R = 20$ Hz the deformation mode depends on the type of eccentricity. This is due to the enormous difference in the magnitude of the force excitation for this order. For a significant portion of dynamic eccentricity the mode is of 1st order and therefore severe critical. This mode causes mechanical damage due to the pulsating excitation of the foundation of the IM. For the centric and static eccentric model the detected main mode is of 4th order and very low magnitude.
Although static eccentricity results in minor extra force excitation the deformation expressed by the level of the body-sound index reaches highest value throughout the spectrum. This is except for the level at rotor speed which is boosted by dynamic eccentricity. The highest values are reached for the order at $f_{36} = 720$ Hz which is the first stator-slot harmonic. Next to the order at rotor speed in case of dynamic eccentricity the largest raise of the body-sound index-level is at $f_{52} = 1040$ Hz. This will result in extra acoustic noise, since the human ear is very sensitive in this frequency range of 1000 to 5000 Hz.
In this paper it is stated and shown, that eccentricity leads to significant extra noise. Static eccentric positioned rotors represent the worst case. Dynamic eccentricity causes excitations with rotor speed and elliptical deformation modes.

References

[1] M. J. DeBortoli, S. J. Salon, D. W. Burow, C. J. Slavik, *Effects of rotor eccentricity and parallel windings on induction machine behavior: A study using Finite Element analysis*, IEEE Transactions on Magnetics, vol. 29, pp 1676-1682, 1993.

[2] J. Rusek, *Diagnostic oriented computer model of the induction machine, accounting for eccentricities and slotting*, 2nd International Seminar on Vibrations and Acoustic Noise of Electric Machinery, VANEM, Łódź, pp 75-79, 2000.

[3] A. Tenhunen, *Electromagnetic forces acting between the stator and eccentric cage rotor*, PHD-Thesis, Helsinki University of Technology, Department of Electrical and Communications Engineering, Laboratory of Electromechanics, Picaset Oy, 2003.

[4] G. Arians, T. Bauer, C. Kaehler, W. Mai, C. Monzel, D. van Riesen, C. Schlensok, *Innovative Modern Object-Oriented Solving Environment - iMOOSE*, www.imoose.de, Aachen, 2005.

[5] C. Schlensok, G. Henneberger, *Comparison of static, dynamic and static-dynamic eccentricity in induction machines with squirrel-cage rotors using 2D-transient FEM*, COMPEL, vol. 23 no. 4, pp 1070-1079, 2004.

[6] J. P. A. Bastos, N. Sadowski, *Electromagnetic Modelling by Finite Element Methods*, Marcel Dekker, Inc., New York, Basel, 2003.

[7] I. N. Bronstein, K. A. Semendjajew, *Taschenbuch der Mathematik*, 4. Auflage, Verlag Harri Deutsch GmbH, Frankfurt am Main, 1999.

[8] C. Schlensok, A. J. Kelleter, K. Hameyer, *Skew-discretization error for structure-dynamic finite-element simulations of electrical machines*, 15th Conference on the Computation of Electromagnetic Fields, COMPUMAG, Shenyang, Liaoning, China, 2005.

[9] H. Jordan, *Der geräuscharme Elektromotor*, Verlag W. Girardet, Essen, 1950.